2008

Temperature and magnetic field dependence of the electronic excitations in the nickel chain compound NINO

Lucas LaViolet
Colby College

Temperature and Magnetic Field Dependence of the Electronic Excitations in the Nickel Chain Compound NINO

Lucas A. LaViolet

Department of Physics and Astronomy
Colby College
2008

Abstract

Temperature and magnetic field dependent absorbance spectra were taken on the Ni^{2+} chain compound NINO ($Ni(C_3H_{10}N_2)_2NO_2(ClO_4)$) in the range from 8,500 to 25,000 cm^{-1}. The identification of an effective C_{4v} symmetry about the nickel ions is supported by assignment of the low temperature absorbance bands. The intensity of many bands is found to be temperature dependent, and in several bands, a shift to higher energy is observed at lower temperatures. A correlation is noted between the field dependence of the spin forbidden electronic transitions and the magnetic properties of NINO. Below a crossover magnetic field, $H_c \approx 10$ T, the absorbance is nearly constant; above H_c, the intensity of the spin forbidden transitions decreases linearly with increasing field. A qualitative explanation for the suppression of the spin forbidden transitions above H_c is suggested.

Contents

List of Figures

Acknowledgments

I would like to offer my sincere thanks to my advisor, Professor Virginia Long, for her patience and willingness to help during the long process of researching and writing this thesis. Without her meaningful evaluation of its many drafts, this paper would not have been completed. In addition to my thesis work at Colby, I consider myself fortunate to have gained hands-on experience while working with her at NHMFL this past JanPlan. Moreover, I have benefited from our thought-provoking physics discussions, and took pleasure in our many conversations that had nothing to do with the classroom.

I. Introduction

Much research has been devoted by Long *et al*. to the study of a group of Ni^{2+} compounds with similar electronic excitations.[1] NENP ($Ni(C_2H_8N_2)_2NO_2(ClO_4)$) and isostructural sister compounds NENB ($Ni(C_2H_8N_2)_2NO_2(BF_4)$) and NTNB ($Ni(C_3H_{10}N_2)_2NO_2(BF_4)$) have been studied to determine the temperature and magnetic field dependence of their optical properties. This paper will present the temperature and magnetic field dependent absorbance spectra of a fourth, closely related compound, NINO ($Ni(C_3H_{10}N_2)_2NO_2(ClO_4)$), which will complement the previous work. The long range goal is to highlight similarities and differences among the members of this group of nickel compounds.

Structure

The crystal chain structure of NINO[2] can be seen in Figure 1, where the hydrogen atoms have been omitted for simplicity. Perchlorate (ClO_4^-) counter ions, which separate the chains comprised of Ni^{2+} ions bridged by nitrite groups (NO_2^-), are likewise absent from the figure because they are along the *c*-axis, which points out of the page. Also bonded to each nickel ion, in an approximate plane, are two trimethylenediamine rings ($C_3H_{10}N_2$).[3] The three related nickel compounds are structurally very similar to NINO,[4] differing only by the type of counter ion isolating the chains (BF_4^- in NENB and NTNB) or the organic rings bonded to each nickel ion (ethylenediamine ($C_2H_8N_2$) in NENB and NENP).

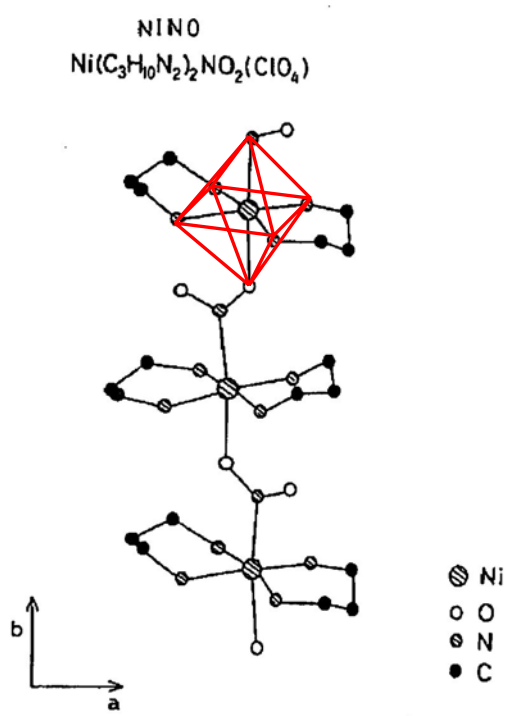

FIG. 1. The crystal chain structure of NINO with the hydrogen atoms omitted for clarity. The six ligand atoms surrounding each nickel ion form the vertices of an approximate octahedron. Perchlorate ions, which isolate the chains, are not visible in this view because they are along the *c*-axis (out of the page). Figure from Takeuchi *et al*.[2]

As illustrated in Figure 1, the six ligand atoms that surround each nickel ion form the vertices of an approximate octahedron. In the results section of this paper, however, we will confirm that the effective symmetry about each nickel ion is actually C_{4v}, slightly lower than octahedral. In fact, due to a lack of perfect symmetry about *any* axis,[3] the molecule belongs to the C_1 point group,[5] although the effective symmetry is found to be somewhat higher.

Magnetic Properties

Despite the structural similarities among the group of four Ni^{2+} chain compounds, the magnetic behavior of NTNB differs from that of the others. In fact, it was the

unexpected apparent behavior of NTNB as a spin glass[6] that motivated the study of this set of four nickel complexes. The remaining three compounds, including NINO, are Haldane compounds, and are therefore made of spin = 1 antiferromagnetic chains. In NINO, as in all Haldanes, there exists an energy gap between the correlated ground state (singlet, spin = 0) and the first excited state (triplet, spin = 1) of approximately 1 meV.[2] It is possible to close this gap by an applied magnetic field, H, because the Zeeman effect causes the three degenerate energy triplet states to split with increasing field, as shown in Figure 2. At the crossover field, H_c, the lowest energy sublevel of the excited triplet becomes the ground state, and the system can gain an induced magnetic moment if the field strength exceeds H_c. Magnetization measurements are designed to determine the induced magnetic moment as a function of applied magnetic field. As shown in Figure 3,

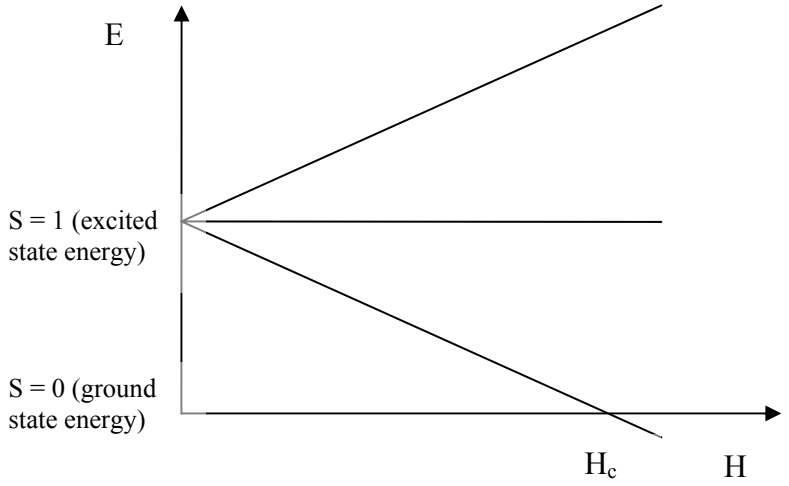

FIG. 2. This schematic diagram shows the energy of the spin states versus the applied magnetic field H. An energy gap on the order of 1 meV exists between the ground state and the first excited triplet state of NINO in the absence of a magnetic field.[2] Zeeman splitting of the triplet state energies in an applied field causes the lowest triplet level to become the lowest energy state at the crossover field, H_c. Below H_c the spin = 0 system cannot be magnetized, but above H_c the system gains an induced magnetic moment as the field is increased.

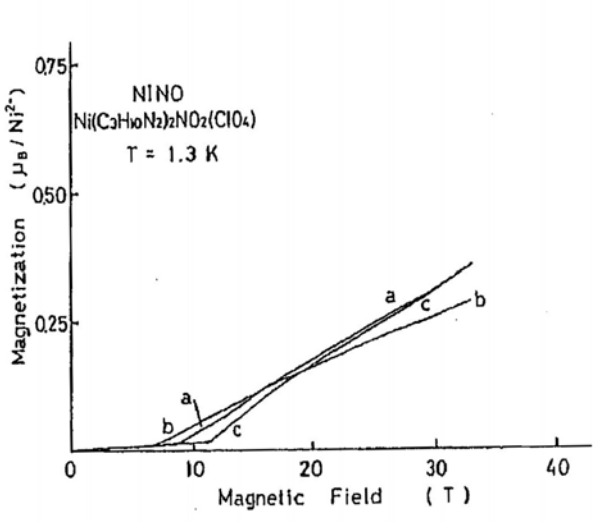

FIG. 3. The magnetization of NINO as a function of magnetic field for the three principal crystal axes. Below the crossover field, the magnetization is approximately zero; thereafter, the magnetization increases linearly with magnetic field. The average crossover field value for the three axes is approximately 10 T. Figure from Takeuchi *et al*.[2]

Takeuchi *et al*. have provided values of the crossover magnetic field for the three principal crystal axes in NINO.[2] The average crossover field value for the three axes is approximately 10 T.

Electronic Transitions

Electronic transitions are produced by the absorption of light. When the difference between the energy level occupied by an electron and a higher potential energy level is equal to the energy of an incident photon, the electron can be excited to the higher energy level.[5] It is possible for multiple energy levels to have the same orbital quantum number. For instance, the presence of ligand atoms around a central ion with electrons in the d orbital ($\ell = 2$), like the Ni^{2+} ions in NINO, causes the five degenerate energy levels of the d orbital to split because the repulsion from ligand anions is greater for electrons in the outer energy levels.[7] As a result of this splitting, a d-d transition can occur, during

which an electron is excited to a higher energy level within the d orbital. Another type of electronic excitation is when a charge is transferred from the central ion to the ligand atoms, or vice versa. The likelihood of such a charge transfer is governed by the overlap of the wave functions for the two sites.[8]

Our goal was to investigate the electronic transitions and their dependence on the parameters of temperature and magnetic field. In molecular compounds such as NINO, electronic transitions are localized on atomic or molecular sites[9] and when electrons are excited from one energy level to a higher energy level, these excitations are governed by selection rules. This section will discuss both the electric dipole and the spin selection rules as they relate to Ni^{2+} ions. In addition, we will consider mechanisms that allow forbidden transitions to appear in the spectrum.

Electric Dipole Selection Rule

The electric dipole selection rule can be expressed in many ways. Put simply, in order for light to be absorbed, there must be a change in the electric dipole moment of a molecule.[10] The dipole moment is intricately tied to the symmetry of a molecule; if the ground state of a given molecule is centrosymmetric about an inversion center, then the electron distribution has no distinct orientation and the molecule has no dipole moment. For example, the electron cloud for an s orbital configuration is spherical and therefore symmetrical about its center. An ion with an outer electron in an s orbital will have no electric dipole moment. For a transition from this state to be allowed, the final state must have a nonzero dipole moment. One such allowed transition is to a p orbital, whose electron cloud is anti-symmetric, and therefore has a dipole moment. The transition from

an s to a p orbital results in a change in the orbital quantum number, ℓ, since the initial value of ℓ is zero (s orbital) and the final value is one (p orbital). The generalization of this example states the electric dipole selection rule mathematically as $\Delta\ell = \pm 1$. Another reformulation of the selection rule, called the Laporte rule, states that transitions that preserve the parity of a molecule with respect to an inversion center are forbidden.[11] This formulation implies that the molecule in question must have a definite parity for the selection rule to apply. The term "forbidden" can be explained by the fact that the intensity of an electric dipole allowed transition is proportional to the magnitude of the change in the electric dipole.[10] Hence a forbidden transition means that the change in the dipole moment is so small that the excitation is too weak to be observed.

In anisotropic samples, the electronic transitions may likewise be anisotropic. A change in the charge distribution from the ground state of a molecule to an excited state must cause a change in the dipole moment that is in the same direction as the oscillating electric field of the electromagnetic wave.[10] Consequently, polarizers can be used to orient the oscillating field so that the dipole moment can be changed in the direction of a chosen axis. For a completely isotropic molecule, the same absorption should occur along any of the axes of symmetry, but because most molecules have some anisotropy, a difference is observed between various orientations.[8] Thus, the spectrum taken when the light is aligned parallel to the length of the crystal chain may have different features than when the chain direction is perpendicular to the incident light.

Spin Selection Rule

The absorption of a photon does not affect the spin of an electron, so the spin should not change between the ground and excited electronic state.[5] This is an expression of the spin selection rule, which states that for an allowed transition, the net change in spin state for an atom must be zero, expressed mathematically as $\Delta s = 0$. For example, the ground state of Ni^{2+}, which has a $3d^8$ electronic configuration, is spin = 1 because the eight electrons in the outermost d orbital are arranged as shown schematically in Figure 4 (a). As required by Hund's rules,[12] there are three paired sets of electrons and then two unpaired electrons of the same spin orientation, chosen arbitrarily to be spin up. One of the paired electrons can make an allowed transition to a

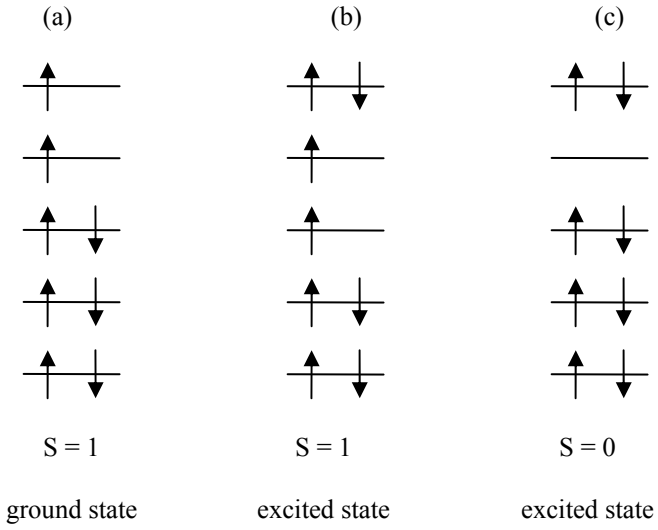

FIG. 4. The eight electrons in the 3d orbital of the Ni^{2+} ion in the ground state (a) and two excited states (b) and (c). A transition from (a) to (b) is allowed by the spin selection rule because the total spin is unchanged during the transition. Transitions from (a) to (c) are forbidden by the spin selection rule because the net change in the spin state is not zero.

higher orbital level so the excited state is as shown in Figure 4 (b). In this case, two orbital levels still have unpaired spin up electrons, and the total spin for the excited state

is again spin = 1. If, however, as shown in Figure 4 (c), the lower of the two unpaired electrons in the ground state was excited to the highest orbital level occupied by the other unpaired electron, the Pauli Exclusion Principle states that the two electrons must have opposite spin orientations.[13] Thus, the transition just described to the spin = 0 state illustrated in Figure 4 (c) is said to be spin forbidden, because the final spin state of the system is different from that of the ground state.

Mechanisms that Allow Forbidden Transitions

Although the electric dipole selection rule forbids all d-d transitions in a centrosymmetric complex (since $\ell = 2$ for all d orbitals), such forbidden transitions are often observed in a variety of molecular compounds.[5] Given that the selection rule applies only to centrosymmetric complexes, any (even temporary) distortion of the structure that causes a change in parity will allow transitions to take place.[10] As mentioned in the section on structure, NINO has no actual center of symmetry, but we seek to determine what effective symmetry governs the behavior of the transitions. If NINO has no effective center of symmetry, we expect to see evidence of d-d transitions in the spectra of our samples. On the other hand, if NINO behaves like a centrosymmetric molecule, a d-d transition will not occur unless a temporary distortion, such as an odd vibration, breaks the symmetry of the complex and induces an electric dipole moment. If an odd (symmetry-breaking) vibration occurs at the same time as the forbidden electronic transition, then the d-d transition becomes weakly allowed. This process is known as vibronic coupling, and the band intensity of the vibronically

activated transition is known to be dependent on the temperature, T, as described by the relation[10]

$$\text{Intensity} \propto \coth\left(\frac{h\nu}{2kT}\right), \qquad \text{Eq. 1}$$

where ν is the frequency of the odd vibration, and h and k are the Planck and Boltzmann constants, respectively. Inspection of this relation reveals that the intensity of the transition increases with temperature, which is consistent with a greater occurrence of vibrations at higher temperatures.[8]

In general, spin forbidden transitions are far less likely than spin allowed transitions, although they can occur by means of either a spin orbit coupling or spin exchange mechanism. The phenomenon of spin orbit coupling occurs because the spin angular momentum and the orbital angular momentum of a particle are not independent.[13] Coupling of the two types of momentum in the cation Ni^{2+} results in a mixed spin state that is neither a pure spin = 0 nor a spin = 1 state. Thus the spin selection rule does not rigidly apply, and a small intensity peak exists in the spectrum where the spin forbidden transition is weakly allowed. A spin forbidden peak is said to borrow some of its intensity from a nearby allowed band in such a way that the strength of a spin forbidden transition to the state with energy E_{SF} in the neighborhood of a spin allowed band with energy E_{SA} is given by[14]

$$\text{Intensity} \propto \frac{1}{(E_{SF} - E_{SA})^2}. \qquad \text{Eq. 2}$$

Consequently, the intensity borrowing is weaker for two states far apart in energy.

The other mechanism that permits spin forbidden transitions is spin exchange. Coupling between nearby magnetic ions can change the total spin of the ground or

excited state.[15] In the case of an isolated Ni^{2+} ion, a transition from the ground state (spin = 1) to a spin = 0 excited state is forbidden. Nevertheless, coupled ions like those in the correlated ground state of Ni^{2+} Haldane compounds are collectively in a spin = 0 state, and the transition to an excited spin = 0 state becomes allowed weakly, depending on the strength of the spin coupling. In isolated atoms, there is no spin exchange since there are no nearby ions with which to couple. In such isolated ions, any spin forbidden transitions that occur must be due to spin-orbit coupling. In a chain such as NINO, however, the spin forbidden transitions could be due to either spin-orbit coupling or spin-exchange.

II. Experimental Procedures

Transmittance spectra were measured to determine the electronic excitations of the NINO samples in the near infrared (NIR) and visible regions (8,500 to 25,000 cm^{-1}). Room temperature optical measurements were taken using Colby's Bruker IFS66V Fourier transform spectrometer. The temperature dependence of the NINO absorptions was then determined for a range from 6 to 300 K using a cryostat insert in the Bruker spectrometer. Low temperature magnetic field dependent measurements were made at the National High Magnetic Field Laboratory in Tallahassee, Florida, using a McPherson grating spectrometer. The details of each type of measurement will be discussed below.

All NINO samples were grown in solution by the slow evaporation method as previously described by Takeuchi *et al*.[2] and provided by Chris Landee of Clark University. The dark red crystals were cleaved into smaller pieces with dimensions on the order of a few millimeters per side and thickness varying by sample from 0.5 to 1 mm. Rubber cement was used to mount the samples onto holders with a circular hole approximately 1.5 millimeters in diameter in such a way that light would pass through the hole perpendicular to the long dimension of the crystal. Based on previous crystal axis assignments,[2] it is assumed in this paper that the crystal chains are perpendicular to the length of the crystal, although this has not been confirmed experimentally for our samples.

Temperature Dependent Measurements

To measure the transmittance in the NIR and visible regions at Colby College, a mounted sample was placed inside a Fourier transform spectrometer. The unique feature inside this type of spectrometer is the Michelson interferometer, which creates a known optical path difference between two split parts of a beam of light. For a typical schematic diagram of such an interferometer, refer to the text by Halliday, Resnick, and Walker.[16] A beam splitter, or half-silvered mirror, is used to divide the light emitted from a source into two beams. One beam travels to a fixed mirror and back. The other beam reflects off a moving mirror so that when the two parts of light reunite, the intensity of the recombined beam recorded as a function of the optical path difference creates an interferogram. A path difference of an integer multiple of the wavelength results in constructive interference, whereas a half-integer multiple of the wavelength results in destructive interference. For example, the interferogram produced by a single wavelength source, such as a laser, would look like a cosine wave, with maximum intensity for a path difference of zero and integer multiples of pi. All Fourier transform spectrometers, however, use a broadband source so that transmittance data can be measured for all wavelengths at the same time. Since a zero path difference results in a maximum intensity for light of any wavelength, a broadband source has a center burst where all wavelengths interfere constructively and wings on either side of the center burst where the wavelengths undergo deconstructive interference.[17]

In order to regain the spectral information, the computer numerically performs an inverse Fourier transform on the interferogram to give a single beam spectrum, which is a plot of intensity versus wavenumber. Wavenumber (cm^{-1}) is a common spectroscopic unit and is proportional to frequency and energy. Scans are taken both with and without

the sample in place, producing a sample and a reference single beam spectrum, respectively. The computer then calculates the transmittance by dividing the sample spectrum by the reference spectrum so that all features in the plot are due to the sample and not artificially caused by the optical components of the instrument.[17] A plot of transmittance versus wavenumber can easily be converted to an absorbance plot by applying to each transmittance point the equation[18]

$$\text{Absorbance} = -\ln(\text{Transmittance}). \qquad \text{Eq. 3}$$

To ensure the best spectral results, we maximized the signal-to-noise ratio before each measurement. Whereas the noise level due to detector fluctuations remains constant, the signal level depends only on the light incident on the detector. Too much light can saturate a detector, but too small a signal count results in overly noisy spectra. Translation stages within the spectrometer made it possible to adjust the sample position so as to optimize the amount of light penetrating the sample. The signal count was also optimized by changing the size of the aperture, to allow more or less light to pass through the sample to the detector. When necessary, an optical filter was added to the setup to block some light and prevent the detector from saturating.

To further improve the signal-to-noise ratio, multiple scans were taken and averaged, which took considerably more time than the mere seconds or less for a single scan. The choice of resolution setting could also increase the total time needed to complete a measurement. Improving the resolution by a factor of two, for example, requires that the moving mirror travel twice as far for each scan. For the majority of the transmittance measurements in the NIR and visible regions, 32 scans were taken at a resolution of 16 cm^{-1}. With these parameters, the total scan time was no more than

approximately 15 seconds using the scanner velocity appropriate for the silicon diode detector.

As stated in the introduction, for a perfectly isotropic molecule, incident light polarized along any of its three crystal axes produces the same absorbance spectrum. In order to detect the anisotropy of our NINO samples, polarized measurements were taken with the oscillating electric field oriented either perpendicular or parallel to the Ni^{2+} chains. Once the polarizer is in place between the source and the sample, the angle of polarization can be changed automatically by a polarizer rotator controlled by the software to find the maximum or minimum transmittances corresponding to the two polarizations. With the correct angles determined, transmittance spectra were measured on three different NINO samples at room temperature in the NIR-visible region at both polarizations. In order to complete the polarized measurements in the full range from 8,500 to 25,000 cm^{-1}, two thin film polaroid polarizers were necessary, one each in the NIR and visible regions, due to their limited functional ranges.

Measuring the transmittance of three NINO samples at room temperature allowed us to make a comparison of the three samples and determine the preferred samples for low temperature and magnetic field dependent measurements. Typically the thinnest sample is the best choice for zero field measurements, since the most light can pass through it, whereas a slightly thicker sample often produces the best results in higher magnetic fields because the change due to the magnetic field is a larger percentage of the total signal.

The low temperature measurements necessitated some additional equipment than that which was required for the room temperature measurements. To cool the system, a

continuous flow cryostat was attached to the sample chamber of the spectrometer. A custom Janis cryostat sample holder was used that could accommodate two identical sample plates. A NINO crystal sample spanned the hole of one plate, while the reference hole was left uncovered. With the holder inside the cryostat, translation stages in all three directions allowed us to switch between centering the light beam either on the sample or the reference hole without removing the sample. A set of windows in the cryostat allowed light from the source to pass through the sample and continue on to the detector.

Before the cooling process could begin, the cryostat and sample chamber were evacuated with the sample holder in place inside. A transfer line was then connected to the cryostat and lowered very slowly into a dewar filled with liquid helium. Inserting the room temperature transfer line too quickly would boil off liquid helium and force us to release the buildup of gas inside the dewar, thus wasting the expensive liquid. The temperature around the sample was monitored by two thermometers, one on the sample holder and the other where the cold gas entered the sample chamber of the cryostat. Within approximately half an hour of beginning to lower the transfer line, the two thermometer readings agreed to within 2 K that the sample chamber was cooled to approximately 6 K.

With the intended temperature reached, the position of the reference hole was optimized using the translation stages. A reference scan was taken after the reference hole was positioned such that the maximum number of counts was read by the detector. The translation stages were then used to move the sample into the path of the light and position it so that the number of counts was again maximized, at which point sample

scans were taken. When satisfactorily reproducible results were attained at that temperature, the sample chamber was slowly heated in 50 K steps, with transmittance measurements being taken and repeated at approximately 6, 50, 100, 150, 200, 250, and 300 K (room temperature). The temperature was controlled inside the cryostat with a heater that balanced its heating power with the cooling power of the helium flowing from the dewar such that the target temperature was reached and kept constant.

Magnetic Field Dependent Measurements

In order to measure the magnetic field dependence of electronic excitations in NINO in fields up to 30 T, a week was spent at the National High Magnetic Field Laboratory (NHMFL) in Tallahassee, Florida. All data were collected at low temperature (approximately 4 K), but the cooling process was somewhat different from that at Colby College. With a NINO sample in place at the end of a long sample probe, the probe was encased by a long cylindrical airtight "can". This can was evacuated and subsequently filled with a small amount of helium exchange gas, and then slowly lowered into a cryostat filled with liquid helium. The exchange gas allowed the sample to attain the same temperature as the liquid helium bath. A liquid nitrogen bath surrounding the cryostat slowed the evaporation of the liquid helium and reduced the number of helium refills necessary in a work day. When a refill was required, a transfer line was gradually let down into a dewar filled with liquid helium. The other end was not inserted into the cryostat until the entire transfer line was cooled and the gaseous outpour of helium exiting the transfer line liquefied. Once the helium level was replenished, the transfer line was removed and the cryostat resealed with rubber stoppers. In contrast to the

helium refill, topping off the liquid nitrogen was a simple process consisting of pouring the fluid from a small dewar directly into the open bath of nitrogen and covering it with some cloth rags.

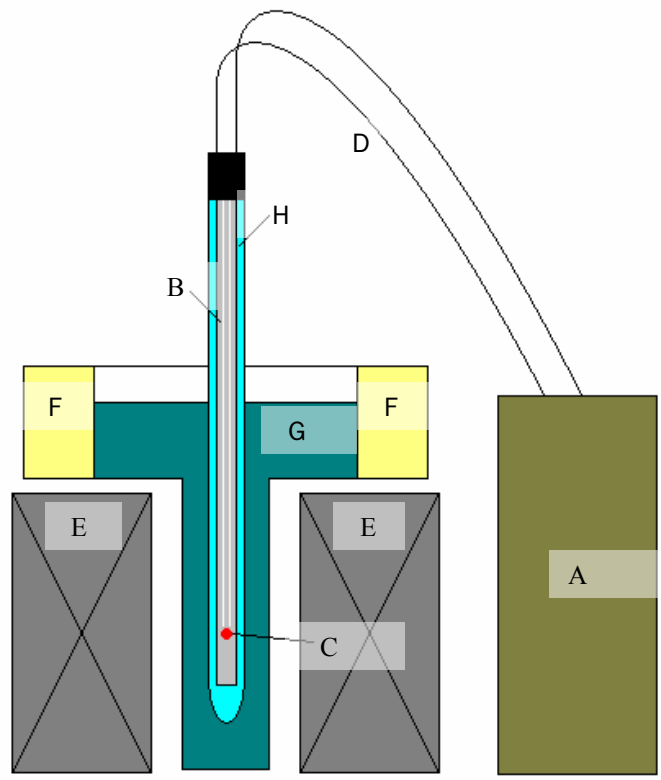

FIG. 5. A cross section of the basic magnet setup for measuring magnetic field dependent absorbance difference spectra at NHMFL. Light travels from a source inside the spectrometer (A) and down the length of the probe (B) to the sample (C) and back to the detector via optical fibers (D). A large magnet coil (E) surrounds the probe. The system is cooled using both a liquid nitrogen bath (F) and a liquid helium bath (G). A small amount of helium gas (H) is used as an exchange gas to transfer heat from the sample probe to the surrounding liquid helium.

Figure 5 shows the basic setup used for transmittance measurements at NHMFL and the details of the cryogenic system described above. The cryostat was positioned inside a large superconducting coil magnet and away from the spectrometer. The physical separation between the light source and the sample was only allowed by the use

of optical fibers that ran from the spectrometer, down the sample probe to the sample, and back to the detector. Two different probe types, Faraday and Voigt, were used to obtain transmittance measurements, with the magnetic field applied perpendicular or parallel to the sample face, respectively. No distinct differences were observed in results obtained by the two geometries. Before measuring a spectrum with the Voigt probe, a vertical translation stage was utilized to adjust the height of the sample in the cryostat relative to the optical fibers, until a maximum number of counts was achieved. No such optimization process could be done on the Faraday probe because the fibers were fixed in place.

The spectrometer available at NHMFL was a McPherson grating spectrometer and thus functioned quite differently than the one used at Colby College. Unlike a Fourier transform spectrometer, a grating spectrometer has no interferometer, and instead relies on a grating to separate light into its component wavelengths. Most grating spectrometers have a small exit slit to allow only a very narrow range of wavelengths of light to be incident on the detector, thus requiring the spectrometer to step through every wavelength in the desired range, with step size determined by the desired resolution.[19] The spectrometer used at NHMFL, however, made use of a charge-coupled detector (CCD), which was calibrated to simultaneously detect a range of wavelengths across 1,024 pixels. This range was determined by the specifications of diffraction grating, the width of the slit through which light entered the spectrometer, and the choice of a center wavelength. A grating of 150 lines per millimeter was used for all transmittance measurements, and the slit width was varied from approximately 100 to 500 micrometers, depending on the other parameters and the desired resolution. Since the resolution was

inversely proportional to the slit width, a narrower slit was sought for higher resolution measurements, with the caveat that enough light ultimately reached the detector to produce a decent signal count. Even with the use of the CCD, it was necessary to overlap four smaller spectra in order to observe the entire region from 8,500 to 25,000 cm^{-1}.

Our goal at NHMFL was to observe the effect of an applied magnetic field on the electronic excitations in NINO. Instead of dividing a sample scan by a reference scan, a high field transmittance measurement was divided by a correspondent zero field measurement, and a transmittance ratio was determined, which was later converted to an absorbance difference using Equation 3. Since no reference scans were taken, the only time constraint was due to the exposure time of the CCD. When the CCD was exposed to light for a longer time, more signal counts were detected, resulting in a more reliable spectrum. On the other hand, a longer exposure time for each measurement not only took more time, but also increased the chance that a long-term drift in the system could skew the data. Ideally, a large signal count would be acquired in a short exposure time without overexposing the detector. The CCD exposure time for our magnetic field dependent measurements ranged from 0.5 to 30 seconds, depending on the sample and setup.

Transmittance measurements at NHMFL followed a standard procedure to ensure reproducibility of results and stability in the system throughout the course of the measurements. Once a sample was in place inside the magnet and cooled, three zero field spectra were recorded. The magnetic field was then increased in constant steps of 1 T, with a spectrum being taken at each field value up to 30 T. A repeat measurement was taken at the highest field, and then the magnet was slowly ramped back down to zero field, where three final spectra were taken to compare with the original zero field ones.

With satisfactory agreement between all zero field spectra, transmittance ratios were calculated and the changes due to the magnetic field were studied.

Due to unexplained drifts in the system and low signal counts with polarizers in place, no satisfactory polarized transmittance measurements were attained at NHMFL. The signal-to-noise ratio was much improved, however, by removing the polarizers from the beam, which allowed more light to reach the sample. The best sets of unpolarized data were taken on the Voigt probe, and measurements took between approximately 8 and 20 minutes. Longer sets of measurements, with 30 second CCD exposure times, lasted upwards of 40 minutes, taking spectra at all the field steps. Occasionally, the magnetic field would be increased to high field in 2, 3, or 5 T increments for data sets with these longer exposure times, thus saving time by taking fewer measurements.

III. Results and Discussion

In this section we present the temperature and magnetic field dependent absorbance spectra of our NINO samples. We begin by identifying the electronic transition associated with each absorbance peak observed in the zero field temperature dependent spectra. Our observations will help us determine an effective symmetry about the nickel ions in the chains of NINO, which we will show is consistent with the temperature dependence of the absorbance band intensities. We will also account for band shifts to higher energies as the temperature decreases. Lastly, a comparison of the low temperature zero field spectra with the magnetic field dependent spectra will reveal a correlation between the electronic transitions and the magnetic properties of NINO.

Temperature Dependence of the Absorbance Spectra

The polarized temperature dependent absorbance spectra were measured at Colby College using the setup described in the previous section. Figure 6 shows the temperature dependence of the absorbance spectra of NINO for the temperature range from 6 to 300 K in the NIR-visible range, which is the energy range where several Ni^{2+} excitations are known to occur.[10] The polarizer was either parallel (Figure 6, left) or perpendicular (Figure 6, right) to the chains. Five large, distinct absorbance bands are present in the spectra located approximately at 10,000, 13,500, 16,000, 19,000, and 21,000 cm^{-1}, with the second lowest energy large band absent in the parallel orientation. Additional subtle features between 12,000 and 14,000 cm^{-1} can be seen in both orientations. It becomes apparent from the insets, which contrasts just the 6 and 300 K

spectra, that these features become sharper at lower temperatures. Two small peaks at approximately 12,610 and 13,130 cm^{-1} are common to both orientations, and will be of particular interest when comparing the temperature and magnetic field dependent results.

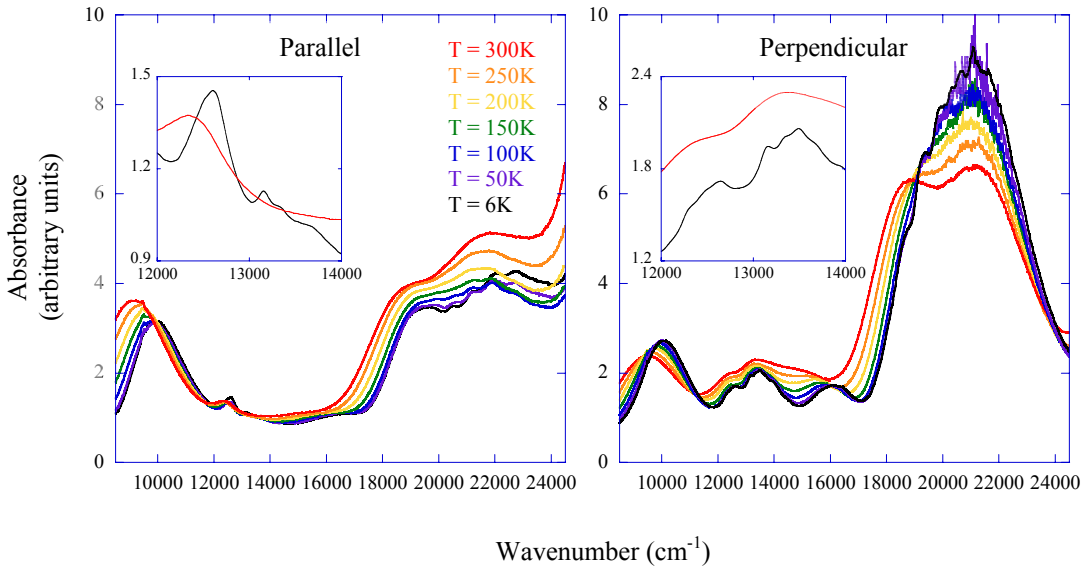

FIG. 6. Temperature dependent absorbance spectra of NINO from 6 to 300 K with the Ni^{2+} chains oriented parallel (left) and perpendicular (right) to the polarizer. Several bands are present, including four spin allowed d-d transition bands approximately centered at 10,000, 13,500, 16,000, and 19,000 cm^{-1} and a charge transfer band around 21,000 cm^{-1}. Many of the d-d bands shift to higher energy at low temperatures, and the intensity of several bands increases with temperature. The insets show that the two spin forbidden d-d transition peaks located at approximately 12,610 and 13,130 cm^{-1} are more prominent at lower temperatures.

Figure 6 also reveals that the center positions of many bands shift to higher energy as temperature decreases. One consequence of this shift is that nearby bands may increasingly overlap. For instance, the fourth band in the perpendicular orientation is centered near 19,000 cm^{-1} at 300 K, but at the lowest temperature, it has shifted such that it lies at approximately the same position as the higher energy fifth band. In contrast to the case of two separate bands, whose respective intensities can be measured by simply

integrating under their curves, the intensities of two overlapping bands add, and it becomes difficult to distinguish the intensity contributions from each band. Due to the overlap of bands in our spectra, integrating directly to find the intensity of any one band and its dependence on temperature is not possible, but we can make some qualitative observations. Based on the fact that the sample is more absorbing at higher temperatures over nearly the entire frequency region in the parallel polarization (left), it is clear that several of the bands have temperature dependent intensities. In the perpendicular orientation (right), the band shift may account for certain changes with temperature, although some band intensities appear to be temperature dependent as well.

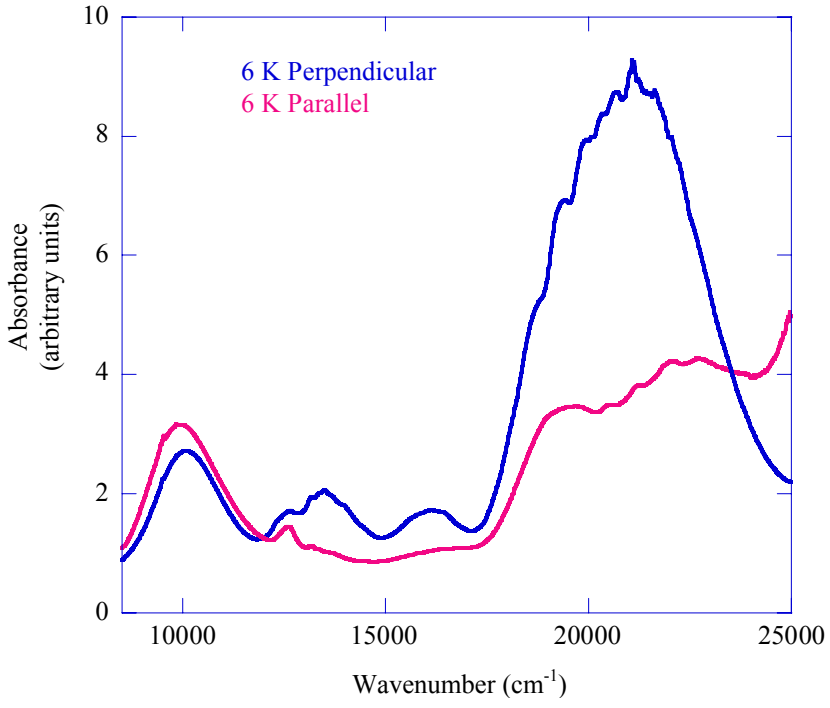

FIG. 7. Comparison of the 6 K perpendicular and parallel polarized absorbance spectra of NINO. Four spin allowed d-d transition bands are visible at approximately 10,000, 13,500, 16,000, and 19,000 cm^{-1}, with the second lowest energy band absent in the parallel orientation. Vibrational fine structure is present on the charge transfer band centered near 21,000 cm^{-1}, with peaks separated by approximately 470 cm^{-1} in the perpendicular orientation and 730 cm^{-1} in the parallel orientation.

By looking at the two polarizations of the 6 K absorbance spectra in Figure 7, we observe that the highest energy band centered at approximately 21,000 cm^{-1} in both the parallel and perpendicular orientations is overlaid with a set of small, evenly spaced peaks known as vibrational fine structure. This fine structure is most apparent in the 6 K spectra because at this low temperature, nearly all of the electrons in the nickel ion are in the lowest vibrational energy level of the ground electronic state. An incident photon may have the minimum energy required for an electron to transition to an excited state plus additional energy to excite a vibration. Since the vibrational energy levels are quantized and evenly spaced,[13] the energy of the absorbed photons is likewise quantized in the same regularly spaced steps, and the low temperature spectra exhibit the vibrational fine structure visible in Figure 7. At higher temperatures, the electrons have sufficient energy to occupy various vibrational levels in the ground state. Therefore there are many more possible energies of photons that can be absorbed, so the fine structure is smeared out.

The presence of vibrational fine structure on this band at 21,000 cm^{-1} gives us clues as to what type of transition produced it. The peak spacing is approximately 470 cm^{-1} in the perpendicular orientation and 730 cm^{-1} in the parallel orientation, which correspond to vibrational frequencies too high to involve the heavy nickel ion.[20] The research literature on Ni^{2+} complexes containing nitrogen-bonded nitrite groups commonly assigns bands located near 21,000 cm^{-1} as charge transfer bands. In most cases, the fine structure has approximately 600 cm^{-1} spacing, and is reportedly due to an electron transfer from the Ni^{2+} to the neighboring NO_2^- group.[21] Additionally, absorbance peaks at approximately 1,325 and 829 cm^{-1} have been attributed to nitrite

vibrations in $NaNO_2$.[10] Since the vibrational frequency of the parallel polarized spectra in NINO is significantly lower than in reported compounds, we suggest that an electron may be transferred instead to a trimethylenediamine ring, which has known vibrations around 450 and 740 cm^{-1}.[22] Regardless of which group is the recipient of the charge, the band cannot correspond to a nickel vibration, so hereafter, we shall refer to this band as the charge transfer band.

To determine the origin of the remaining bands, it will be helpful to consider the possible electronic excitations that can take place within the d orbital of a nickel ion like the ones present in the chains of NINO. The schematic diagram in Figure 8 shows the spin allowed and spin forbidden d-d transitions of $3d^8$ Ni^{2+} in two different crystal field symmetries: octahedral (O_h) and C_{4v}. A complex belonging to the point group C_{4v} possesses only the symmetry of a four-sided pyramid and therefore has fewer symmetry operations than an octahedral complex.[8] As such, we expect the degenerate excited energy levels of an O_h complex to split in the lower C_{4v} symmetry, as shown in Figure 8, where the superscript 1 or 3 on each energy level denotes either a spin = 0 singlet state or a spin = 1 triplet state, respectively. The basic energy ordering of this diagram was taken from a discussion of various C_{4v} nickel complexes by Hitchman.[23] Higher energy excited states are possible for a Ni^{2+} ion, but are left out of this diagram because their energies lie outside the NIR-visible range. Based on the number of absorbance peaks in our spectra, the lower symmetry assignment of C_{4v} is in closer agreement with our observed spectra of Ni^{2+} excitations in NINO. We identify the four remaining large absorbance peaks, centered near 10,000, 13,500, 16,000, and 19,000 cm^{-1}, as the four spin allowed d-d

transition bands, namely, from lowest energy to highest, $^3B_1 \rightarrow {}^3E(1)$, $^3B_1 \rightarrow {}^3B_2$, $^3B_1 \rightarrow {}^3A_2$, and $^3B_1 \rightarrow {}^3E(2)$.

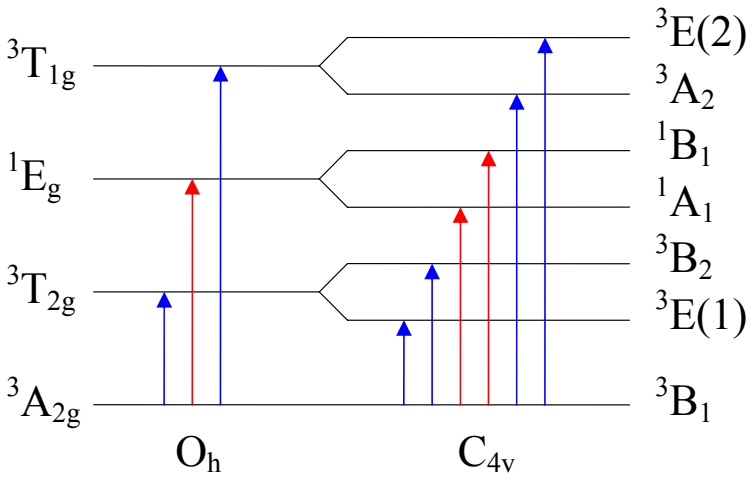

FIG. 8. Schematic diagram of the possible electronic transitions between energy levels of $3d^8$ Ni^{2+} in octahedral (O_h) and C_{4v} crystal field symmetries.[23] Electrons begin in the ground state energy level and make a transition to higher energy levels. Transitions labeled in blue are allowed by the spin selection rule; those labeled in red are spin forbidden. An effective C_{4v} symmetry about the nickel ions in NINO is more consistent with our observed spectra.

The two spin forbidden transitions labeled in the C_{4v} symmetry in Figure 8 can also be accounted for in the temperature dependent spectra. These coincide with the two small absorbance peaks located at 12,610 and 13,130 cm^{-1} in Figure 7, which we therefore identify as the spin forbidden d-d transitions $^3B_1 \rightarrow {}^1A_1$ and $^3B_1 \rightarrow {}^1B_1$, respectively. As mentioned in the introduction, in contrast to an isolated nickel ion, NINO is composed of chains of nickel ions, so the spin forbidden transitions could be allowed by either spin-orbit coupling or spin exchange. Based on the spectra of NINO alone, we cannot attribute the presence of the spin forbidden peaks to one mechanism over the other, but comparison to the spectra of a Ni^{2+} paramagnetic analog to NINO may be useful in distinguishing the contributions due to each.

As a further indication that C_{4v} is the appropriate effective symmetry assignment, a parallel polarized $^3B_1 \rightarrow {}^3B_2$ transition is forbidden by vibronic selection rules in this symmetry group,[23] which may explain the absence of the second absorbance peak in the parallel polarized spectrum. An effective C_{4v} symmetry assignment is also consistent with the known crystal structure of NINO. The bond length from the Ni^{2+} ion to the neighboring oxygen atom of the nitrite group is longer than the bond of the Ni^{2+} to the nitrogen on the opposite nitrite group.[3] The existence of two different bond lengths effectively breaks the mirror symmetry across the plane of the octahedron, leaving the symmetry of a four sided pyramid (C_{4v}). The vertices of such a pyramid consist of the five nitrogen atoms that surround each nickel ion.

Let us consider the temperature dependence of absorbance bands in the two crystal field symmetries. Recall that all d-d transitions are forbidden by the electric dipole selection rule in centrosymmetric complexes, with vibronic activation a necessary mechanism for the transitions to occur, and that vibronic activation implies increasing band intensity with temperature. All d-d transition bands in the spectrum of a complex with O_h symmetry will therefore be sensitive to temperature. In contrast, for a complex in a C_{4v} point group, the two $^3B_1 \rightarrow {}^3E$ transitions for the perpendicular orientation are allowed d-d transitions,[23] and therefore only those bands should be temperature independent. A quantitative comparison of the temperature-dependent band intensities in NINO to the temperature dependence predicted by Equation 1 is thwarted by the considerable overlap of neighboring bands. Nevertheless, we have observed that the intensities of all the d-d transition bands in the parallel orientation increase with temperature, as is expected for vibronically activated bands. In the perpendicular

orientation, the two forbidden transitions ($^3B_1 \rightarrow {}^1A_1$ and $^3B_1 \rightarrow {}^1B_1$) appear to be temperature dependent as well. The second $^3B_1 \rightarrow {}^3E$ transition band overlaps too strongly with the charge transfer band to analyze its temperature dependent intensities. In contrast, the first perpendicular polarized $^3B_1 \rightarrow {}^3E$ transition band has an intensity that is independent of temperature. The fact that the intensity of at least one d-d transition band is temperature independent indicates that the electric dipole selection rule does not apply, thus confirming the noncentrosymmetric point group about the nickel ions.

We will now address the observation that several of the absorbance bands shift to higher energies with decreasing temperature. The observed shift is a result of the fact that materials contract at low temperatures because the average bond length between atoms decreases.[24] If we consider our nickel system as a particle in a box, where the width of the box around the Ni^{2+}, L, is represented by the average bond length between atoms, then we can relate the spacing between energy levels to the temperature dependent bond lengths. The nth energy level of a particle in a box is given by[13]

$$E_n = \frac{n^2 \hbar^2 \pi^2}{2mL^2}, \qquad \text{Eq. 4}$$

where the particle has mass m. Thus at lower temperatures, the smaller average bond length will result in greater separations between energy levels. An electron will therefore require more energy to make the transition to an excited state than at a higher temperature, and the center positions of the absorbance bands will consequently shift to higher energies as the temperature decreases.

Magnetic Field Dependence of the Absorbance Spectra

In Figure 9 we can see the familiar low temperature polarized absorbance spectra from Figure 7 (scaled on the right axis) displayed along with the unpolarized magnetic field dependent absorbance difference spectra (left axis) for easy comparison. The wavenumber range is limited to that for which field dependence was measured. To highlight the magnitude of the changes with applied field, only the highest field and the zero field spectra are shown in red and black, respectively, on this graph. An absorbance difference of zero indicates that the magnetic field had no effect on the ability of the

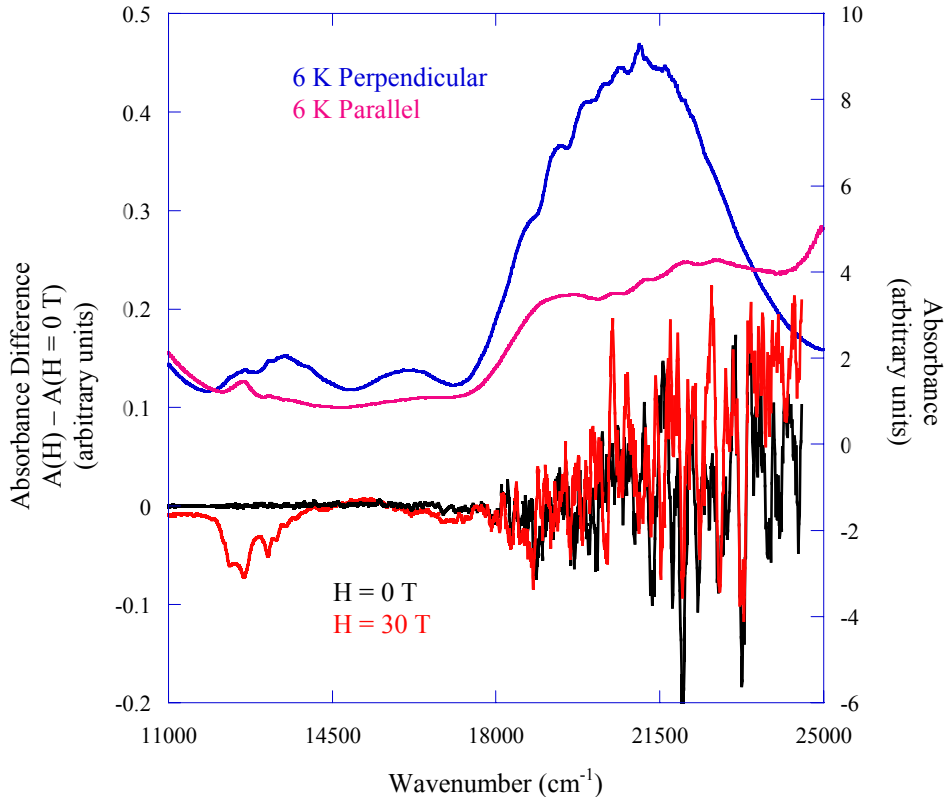

FIG. 9. Overlay of the 6 K polarized absorbance spectra, also shown in Figure 7, (right scale) with the unpolarized low temperature magnetic field dependent absorbance difference spectra (left scale) for 0 T (black) and 30 T (red). The absorbance difference calculated in a field with strength H is equal to the zero field absorbance subtracted from the absorbance at H. The temperature dependent spectra were measured on a separate, thinner NINO sample than the magnetic field dependent spectra.

NINO sample to absorb light. A positive value for the absorbance difference signifies that the sample was more absorbing at higher fields, and a negative value indicates that the field suppressed the absorption of light.

Figure 9 shows that in the frequency region from approximately 11,000 to 14,000 cm^{-1} the absorbance difference decreases at high field. The spectrum exhibits several sharp features in that region, the largest of which constitutes approximately 1-2% of the total absorbance at that point in the zero field spectra. There appears to be no considerable effect from magnetic field at frequencies above 18,000 cm^{-1}. Both the 0 T and 30 T absorbance difference spectra deviate randomly from the 0 line, indicating that the shape likely results from insufficient light striking the detector rather than any feature

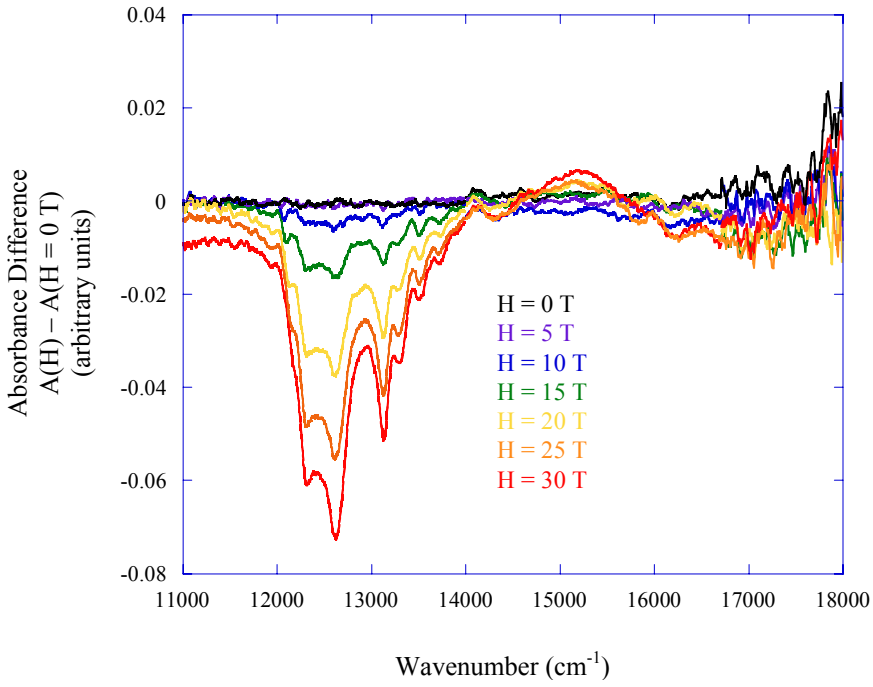

FIG. 10. Absorbance difference spectra for NINO in selected magnetic fields up to 30 T. In the region below 14,000 cm^{-1}, the absorbance of light is suppressed by an applied field, with distinct dips present at approximately 12,610 and 13,130 cm^{-1}.

in the spectrum. The low signal is probably due to the strongly absorbing charge transfer band as well as reduced signal throughput at high frequencies.

An enlarged depiction of the magnetic field dependent results can be seen in Figure 10. Spectra were taken in H = 1 T steps, but only selected ones are shown for clarity. We observe that two sharp dips in absorbance difference occur at 12,610 and 13,130 cm^{-1}, precisely the frequencies corresponding to the two spin forbidden transition peaks. At approximately 12,310 cm^{-1} there is a less pronounced dip in absorbance difference, and three similar features are present at 13,310, 13,510, and 13,710 cm^{-1}.

By making a comparison between the same magnetic dependent absorbance difference spectra and the low temperature zero field absorbance spectra, it becomes apparent that a correlation exists between the magnetic properties and the electronic transitions occurring in NINO. Figure 11 highlights the fact that each dip in absorbance difference corresponds to a feature in the zero field spectra. The three weaker features identified in the previous paragraph are spaced at nearly regular separations of 200 cm^{-1} above the dip at 13,130 cm^{-1}, implying that they may correspond to vibrational replicas of the spin forbidden transition. Likewise, the extra feature near the dip at 12,610 cm^{-1} may be related to a lower vibrational replica of the first spin forbidden transition. It is clear that an applied magnetic field suppresses the absorption of photons corresponding only to the spin forbidden transitions in NINO.

In order to quantify the magnetic field dependence of the spin forbidden transitions, we integrated under the curve from 12,000 to 14,000 cm^{-1} in each absorbance difference spectrum and plotted the integration areas versus magnetic field. The resulting graph is shown in Figure 12. Since the integration area of the absorbance difference is

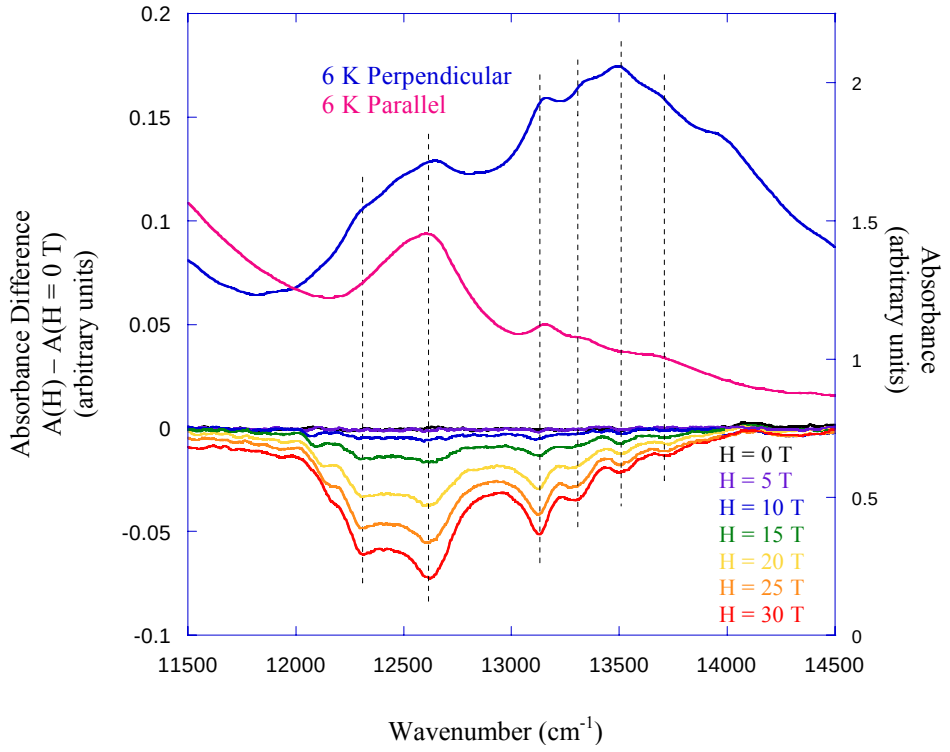

FIG. 11. Overlay of the 6 K polarized absorbance spectra (right scale) with selected unpolarized low temperature magnetic field dependent absorbance difference spectra (left scale) up to 30 T. Each dip in absorbance difference coincides with a peak in the zero field absorbance spectra, where the two sharpest dips at 12,610 and 13,130 cm^{-1} correspond to the two spin forbidden transitions and the other features are related to vibrational replicas of these transitions.

equal to the change in intensity produced by the applied field, Figure 12 illustrates the relation between the absorbance intensity and the magnetic field strength. Below a certain magnetic field value of approximately 10 T, denoted H_c for crossover field, the absorbance intensity is relatively unaffected by the strength of the field. Above this crossover field, however, the absorbance decreases linearly as the field is increased. Recall that magnetization measurements performed on $NINO^2$ (shown in Figure 3) showed a crossover field near 10 T. Also recall that such a crossover field is unique to materials with an energy gap between singlet and triplet magnetic states, whereas most

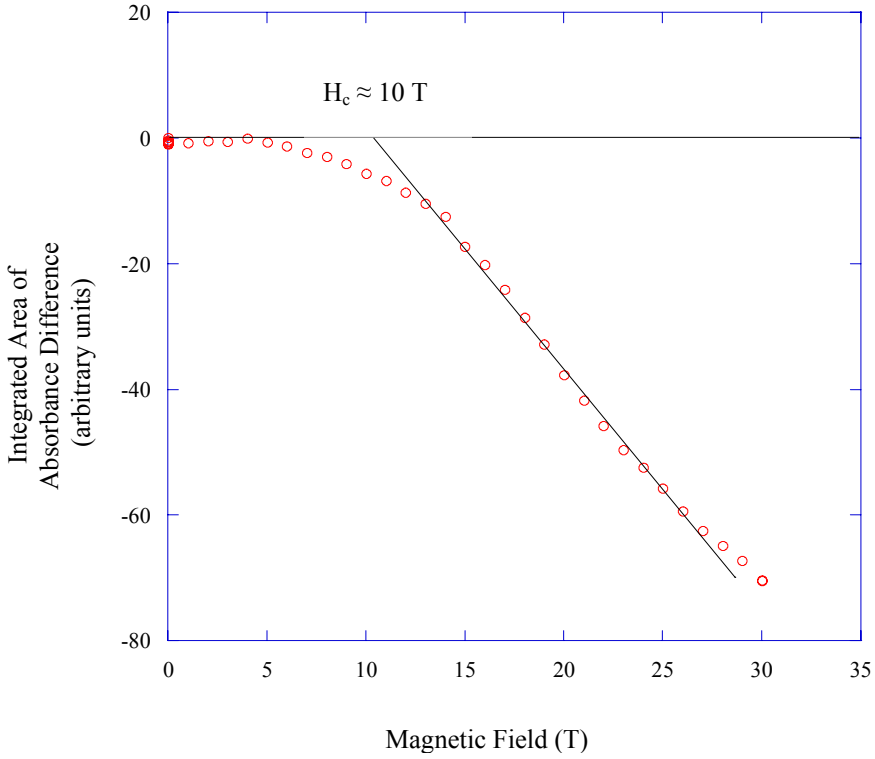

FIG. 12. The integrated areas under the curves of each absorbance difference spectrum of NINO from 12,000 to 14,000 cm^{-1} versus magnetic field. Below a crossover field (H_c) of approximately 10 T, the absorbance intensity is nearly constant; above H_c the absorbance decreases linearly with increasing field. The integration region corresponds to the two spin forbidden peaks, so it appears that the spin forbidden transitions become less likely in higher magnetic fields.

materials respond immediately to an applied field.[1] Thus, it is interesting to note that the spin forbidden electronic transitions in NINO are somehow correlated to the compound's magnetic properties.

We refer to Figure 2 for a feasible qualitative explanation for this connection between the electronic transitions and the magnetic properties of NINO. As described in the introduction, spin exchange causes the correlated ground state of NINO to be a spin = 0 state. Taking this into account, the transitions to the two singlet states $^1A_1$ and $^1B_1$ can be weakly allowed in the spin coupled chain, although forbidden by the spin selection rule on the isolated Ni^{2+} ion. When the lowest energy triplet of the first excited magnetic

state (spin = 1) becomes the ground state at the crossover field, H_c, the transitions to the two spin = 0 states once again become spin forbidden. The intensity of the spin forbidden absorbance peaks could thus be expected to decrease above the crossover field. Admittedly, such a complex system cannot be simplified to this extent. While our speculative description seems to account for the presence of a crossover field in the absorbance difference intensities, it is not clear that it can explain why the spin forbidden transitions are increasingly less likely to occur at fields above H_c.

IV. Conclusion

We have determined the temperature and magnetic field dependence of the electronic excitations for the Ni^{2+} chain compound NINO. Each absorbance band in the NIR-visible region was identified either as a d-d transition band or a charge transfer band. These assignments were in good agreement with an effective C_{4v} symmetry about the nickel ions, which was further supported by the temperature independence of at least one d-d transition band. The effect of an applied magnetic field was restricted to the spin forbidden transitions, which were suppressed by fields above $H_c \approx 10$ T. Without accounting for the linear relation between magnetic field strength and absorbance difference above H_c, a qualitative explanation was suggested for the intensity reduction above the crossover field.

References

1. V. C. Long, Y.-H. Chou, I. A. Cross, A. C. Kozen, J. R. Montague, E. C. Schundler, X. Wei, S. A. McGill, B. R. Landry, K. R. Maxcy-Pearson, M. M. Turnbull, and C. P. Landee, Phys. Rev. B **76**, 024439 (2007).
2. T. Takeuchi, M. Ono, H. Hori, T. Yosida, A. Yamagishi, and M. Date, J. Phys. Soc. Jpn. **61** (1992) 3255.
3. T. Yosida and M. Fukui, J. Phys. Soc. Jpn. **61** (1992) 2304.
4. V. C. Long, Y.-H. Chou, I. A. Cross, A. C. Kozen, L. A. LaViolet, C. A. Miller-Shelley, J. R. Montague, E. P. Plumb, S. A. McGill, X. Wei, B. R. Landry, K. R. Maxcy-Pearson, M. M. Turnbull, C. P. Landee, and R. D. Willett, APS MAR08, New Orleans.
5. D. Sutton, *Electronic Spectra of Transition Metal Complexes*, (McGraw-Hill, London, 1968).
6. R.D. Willett and C. J. Gomez-Garcia, EMRS2007, Strasbourg.
7. S. F. A. Kettle, *Physical Inorganic Chemistry: A Coordination Chemistry Approach*, 1st ed. (Oxford University Press, New York, 1998).
8. B. N. Figgis and M. A. Hitchman, *Ligand Field Theory and Its Applications*, 1st ed. (Wiley-VHC, New York, 2000).
9. J. C. Kotz, M. D. Joesten, J. L. Wood, and J. W. Moore, *The Chemical World: Concepts and Applications*, (Saunders College Publishing, Fort Worth, 1994).
10. A. B. P. Lever, *Inorganic Electronic Spectroscopy*, 2nd ed. (Elsevier, Amsterdam, 1984).
11. P. W. Atkins, *Physical Chemistry*, 2nd ed. (W. H. Freeman and Company, San Francisco, 1982).
12. M. A. Fox and J. K. Whitesell, *Core Organic Chemistry*, 1st ed. (Jones and Bartlett Publishers, Boston, 1997).
13. R. Eisberg and R. Resnick, *Quantum Physics of Atoms, Molecules, Solids, Nuclei, and Particles*, 2nd ed. (John Wiley & Sons, New York, 1985).
14. C. J. Ballhausen, *Molecular Electronic Structures of Transition Metal Complexes*, 1st ed. (McGraw-Hill, London, 1979).
15. H. U. Güdel, *Magneto-Structural Correlations in Exchange Coupled Systems*, edited by R. D. Willett, D. Gatteschi, and O. Kahn (Reidel, Boston, 1985).
16. D. Halliday, R. Resnick, and J. Walker, *Fundamentals of Physics Extended*, 5th ed. (John Wiley & Sons, New York, 1997).
17. *Introduction to Fourier Transform Infrared Spectroscopy*, Thermo Nicolet Corporation, 2001, http://mmrc.caltech.edu/FTIR/FTIRintro.pdf.
18. Absorbance/Transmittance Conversion, LabCog*nition*, Analytical Software GmbH & Co., 2007, http://www.labcognition.com/panoramaonlinehelp/Englisch/mathematics/absorbance_transmittance_conversion.htm.
19. D. C. Giancoli, *Physics: Principles with Applications*, 2nd ed. (Prentice Hall, Inc., Englewood Cliffs, 1985).
20. J.-H. Wang, Z. Cheng, J.-L Brédas, and M. Liu, J. Chem. Phys. **127** (2007) 214705.
21. M. A. Hitchman and G. L. Rowbottom, Coord. Chem. Rev. **42** (1982) 55.

22. E. Kasap and Z. Kantarci, J. Inclusion Phenom. **28** (1997) 117.
23. M. A. Hitchman, Inorg. Chem. **11** (1972) 2387.
24. R. Turton, *The Physics of Solids*, 1st ed. (Oxford University Press, New York, 2000).